



## Pole placement and LQR implementation on longitudinal altitude holding control of wing in surface effect vehicle

Muhammad Nanda Setiawan<sup>a,\*</sup>, Evan Rizky Suryana<sup>b</sup>, Leo Parytta<sup>c</sup>, William Andaro<sup>c</sup>

<sup>a</sup> Department of Renewable Energy Engineering, Universitas Prasetiya Mulya  
BSD City Kavling Edutown I.1, Tangerang, Indonesia

<sup>b</sup> Department of Engineering Physics, Multimedia Nusantara University  
Jl. Scientia Boulevard Gading Serpong, Tangerang, Indonesia

<sup>c</sup> Department of Physics Energy Engineering, Surya University  
F8 & F9 Grand Serpong Mall Jalan MH. Thamrin Panunggan Utara, Tangerang, Indonesia

Received 3 August 2020; Accepted 5 November 2020; Published online 22 December 2020

### Abstract

The longitudinal altitude holding control system (LAHCS) of wing in surface effect (WiSE) vehicle has been developed using Simulink/Matlab. The LAHCS is designed to maintain the altitude of the vehicle stands at 1 m above the surface, with a maximum allowable deviation of 0.5 m. The purpose is to gain an additional lift generated by the surface effect to increase the aerodynamic performance. This control system is investigated using two approaches, i.e., the pole placement and the linear quadratic regulator (LQR) methods. Originally, the system shows an unstable response on the phugoid mode, indicated by the positive value of its Eigen. After the pole placement method is applied, the system is stable and capable of maintaining the reference command altitude. This method produces 0.27 of the maximum altitude deviation when the disturbance, represented by the doublet input elevator  $\pm 5^\circ$  is applied. Moreover, the time needed for the system to reach the steady-state response of altitude is around 2.2 seconds. In comparison, the LQR method is also applied to the system with the same scenario. Although the settling time response is quite similar to the previous result, its maximum altitude deviation is significantly reduced by around 80 %. In conclusion, both of the methods used to design the LAHCS are capable of maintaining the altitude of the WiSE vehicle always below its maximum deviation tolerance.

©2020 Research Centre for Electrical Power and Mechatronics - Indonesian Institute of Sciences. This is an open access article under the CC BY-NC-SA license (<https://creativecommons.org/licenses/by-nc-sa/4.0/>).

Keywords: wing in surface effect vehicle; altitude holding control system; pole placement method; linear quadratic regulator (LQR); phugoid mode; doublet input elevator.

### 1. Introduction

Indonesia is an archipelago country, where most of its territory is dominated by the ocean. Indonesian fishermen utilize the ocean to make a living. Unfortunately, the high amount of illegal fishing carried out by other countries makes local anglers suffer losses. In order to prevent illegal fishing, the Indonesian government conducts monitoring activity around the outermost areas. The surveillance is generally carried out by Indonesian soldiers using a speedboat. However, due to the high density of water, speedboats suffer from high drag, thus limiting their speed and manoeuvrability. High drag also tends to cause higher fuel consumption, especially against the sea waves. So, it is needed to

find alternative vehicles with less fuel consumption to increase the maximum range of the observed area. According to Li and Chen [1], the surface effect of the WiSE vehicle could increase the lift to drag ratio by 40 % - 70 %. Consequently, it does not only reduce the fuel consumption rate significantly but also increases the coverage area. Another study by Amir *et al.* [2] concludes that the WiSE vehicle's capabilities are superior over marine vessels. The WiSE vehicle speed is relatively faster and the CO<sub>2</sub> emission is 20 % lower due to its fuel efficiency.

Due to its advantages, the wing in surface effect vehicle has a potential to be applied to marine surveillance missions in Indonesia. This vehicle utilizes the benefit from the ground effect, which increases the aerodynamic performance (lift to drag ratio). The higher lift to drag ratio represents the higher aerodynamic efficiency, which reduces fuel consumption. In order to gain benefit from the

\* Corresponding Author. Phone: +6221-30450500.  
E-mail address: [nanda.setiawan@prasetiyamulya.ac.id](mailto:nanda.setiawan@prasetiyamulya.ac.id)

ground effect, the WiSE vehicle needs to maintain its altitude always near the surface [3]. However, aerodynamic modelling and stability analysis on the WiSE vehicle is rather more complex than the regular aircraft due to the ground effect. Also, the WiSE vehicles control system plays an important role in flight safety because of the close proximity of the craft to the sea surface. Studies on WiSE vehicle aerodynamic modelling and stability analysis has been done [4][5][6], but studies on the control system are still limited due to its complexity [7][8].

This paper discusses the development of the LAHCS of the WiSE vehicle using pole placement and LQR methods. The control system must be able to maintain the vehicle's altitude around 1 m above the surface, with a maximum deviation of 0.5 m. This is the main requirement for designing the LAHCS. It will guarantee not only the benefits from an additional lift but also to prevent the vehicle from crashing onto the surface.

In the previous research, the development of an automatic flight control system of Wing in Surface Effect Craft (WiSE-Craft) has been conducted by Hari Muhammad *et al.* [9]. The automatic flight control is designed using the gain scheduling method, where the gains are obtained from the root locus diagram. The control system on that research can stabilize the WiSE vehicle both for phugoid and short period modes. They simulate the control performances with three different operational altitudes, defined as 1 m, 2 m, and 3 m. However, the maximum altitude deviation is still high, standing around 0.72 m. It will have a safety issue for lower operational altitude, i.e., 1 m above the surface.

In order to improve the robustness stability of the system, the pole placement and LQR methods are applied to our LAHCS design. The gains parameters

of the pole placement method are calculated based on the Ackermans formula, while the LQR is implemented by setting the weighting matrix Q and R based on the parameters that want to improve. The doublet input elevator is used to simulate the robustness of the system in order to deal with a disturbance. It is defined as a double step input with the amplitude  $\pm 5^\circ$  with 4 seconds period. The flight dynamic equation is constructed with a linear approach by using a longitudinal dynamic equation, where the lateral effect is decoupled based on the small disturbance theory [10][11][12]. To deal with complexity, the thrust parameter is neglected from the equation, hence the speed of the aircraft is assumed to be constant and the input parameter is limited only regarding the elevator deflection. Besides, the WiSE aerodynamic coefficients are calculated using DATCOM+ or XFLR5 program by inputting the vehicle's geometry [13][14].

## II. Materials and Methods

### A. Aerodynamic coefficient

The longitudinal dynamic equation is obtained from the derivation of the WiSE aerodynamic formula, affected by its geometry design. The first model of WiSE vehicle is developed at Surya University. This vehicle is designed to accommodate up to nine passengers, including the pilot. The expected cruise and top speed of the vehicle are 100 km/h and 150 km/h, respectively. Figure 1 describes the 3D model of the WiSE vehicle. The geometry of the aircraft in Figure 1 can be used as an input for the XFLR5 program to extract its aerodynamic coefficients. Moreover, the flight condition variations, i.e., angle of attack, velocity, and altitude also take into account in order to simulate the real condition

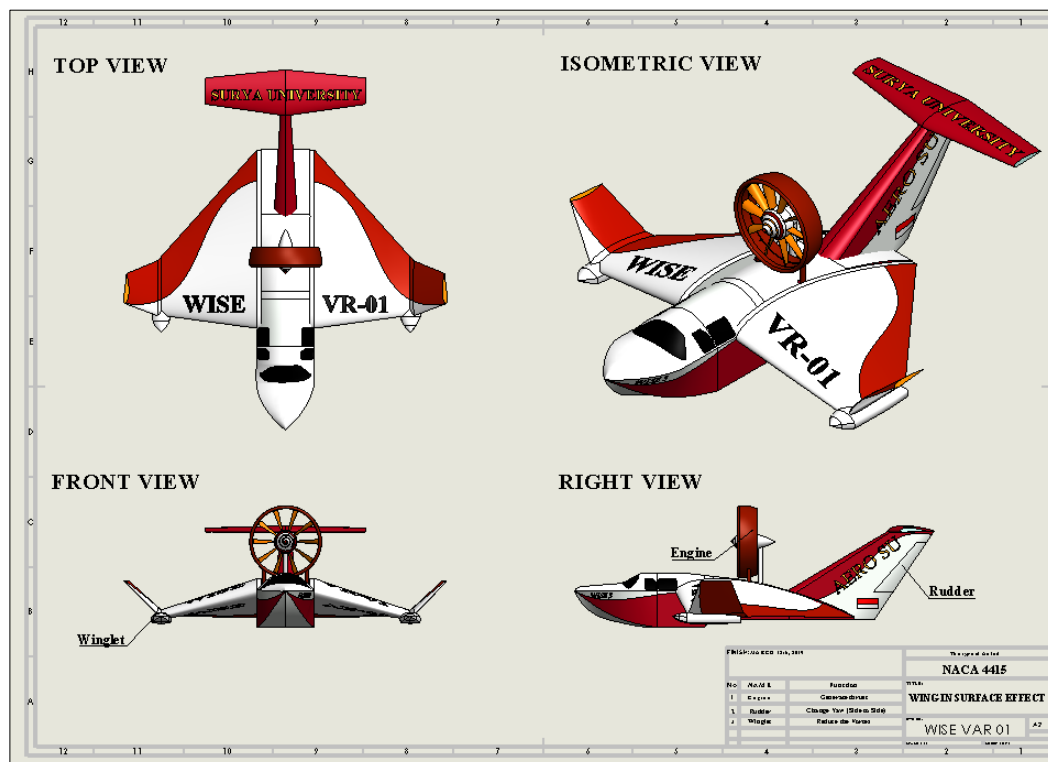


Figure 1. 3D model of WiSE vehicle

Table 1.  
Parameter of the WiSE vehicle

Parameter	Value
Mass, m	1000 (kg)
Mean aerodynamic chord, c	3.28 (m)
Centre of gravity, xcg	28% MAC
Angle of attack, $\alpha$	-6° to 20°
Velocity, $V_0$	100 to 150 (km/h)
Altitude, H	0.5 to 2 (m)
Wing area, $S_w$	19.77 (m <sup>2</sup> )
Horizontal tail area, $S_h$	4.47 (m <sup>2</sup> )
Horizontal tail area, $S_y$	4.38 (m <sup>2</sup> )
Wing span, bw	7.38 (m)
Horizontal tail span, bh	4.45 (m)
Horizontal tail span, by	4.12 (m)
Vertical tail root chord, cr	2.974 (m)
Vertical tail tip chord, ct	1.276 (m)
Horizontal tail arm, lh	3.195 (m)
Vertical tail arm, lv	2.910 (m)
Roll moment inertia, $I_x$	1.396 (kgm <sup>2</sup> )
Pitch moment inertia, $I_y$	6.763 (kgm <sup>2</sup> )
Yaw moment inertia, $I_z$	6.834 (kgm <sup>2</sup> )
Coupling inertia x-z, $I_{xz}$	-1.560 (kgm <sup>2</sup> )
Overall length	10 (m)
Overall height	1.78 (m)
Max. fuselage width	1.6 (m)
Wing dihedral angle, $\Gamma_w$	-9.1°
Wing incidence angle, $\eta_w$	7.81°
HT incidence angle, $\eta_h$	0°
VT sweep angle, $\lambda_v$	54.93°
Wing root airfoil	NACA 4415
Wing tip airfoil	NACA 4415
HT airfoil	NACA 4415
VT airfoil	NACA 0012

of the vehicle while operating. The parameters of the WiSE vehicle used as the baseline system for XLFR5 input are listed in Table 1.

The aerodynamic coefficients extracted from the XLFR5 software are listed in Table 2, where  $C_{X^*}$ ,  $C_{Z^*}$ , and  $C_{M^*}$  stand for the coefficient of axial force, normal force, and pitching moment, respectively. These results are generated based on the data in Table 1. It can be seen that the altitude and the angle of attack

are varied in order to capture all data possibilities regarding the operational condition of the WiSE vehicle. The forces coefficients in Table 2 are distinguished regarding its derivative, i.e., axial velocity, angle of attack, pitch rate, pitch angle, and control surface deflection. In order to get their dimensionless quantities, the values in Table 2 are then submitted to the equations in Table 3, where  $V_0$ ,  $m$ ,  $S$ ,  $\bar{c}$ ,  $I_{yy}$  stand for operational velocity, mass of the vehicle, span of the wing, mean aerodynamic chord, and polar moment of inertia respectively. These equations are used to arrange the longitudinal dynamic equation of the WiSE vehicle by assuming that there is no coupling from the lateral mode and the thrust parameter is neglected. It means that the vehicle's speed is maintained to a steady level (constant) and the longitudinal control relies only upon the elevator [15].

These non-dimensional aerodynamic coefficients are then arranged into the state space equation, which later can be used as a basis of systems improvement with the pole placement and LQR methods. By observing the root locus behaviour of the original system, the feedback gains can be examined based on their transient performances, i.e., maximum overshoot, settling time, steady-state error, etc.

## B. Longitudinal dynamic equation

As discussed in the previous section, the dimensionless aerodynamic coefficients in Table 3 are important in determining the flight behavior of the WiSE in the longitudinal direction. It describes the axial velocity, pitch rate, pitch angle, altitude, and the elevator deflection angle of the aircraft. It should be noted that these results are calculated based on the geometric input of the aircraft. As such, providing the detail of a 3D model of the WiSE vehicles is mandatory; otherwise, the parameters cannot be extracted accurately from the XLFR5. However, to deal with complexity, the engine geometry is excluded from the calculation. For future improvement, the non-dimensional aerodynamic coefficients derivation from the entire aircraft can be calculated using a better

Table 2.  
Aerodynamic Coefficient Calculation Result

Coefficient	Derivative to				
	u	$\alpha$	q	$\theta$	$\eta$
$C_{X^*}$	-0.10652	244.17	-0.000214	-8.41E-05	0.00143
$C_{Z^*}$	-0.013155	5.6533	13.162	5.19	-0.0043
$C_{M^*}$	-0.030233	-2.9563	-36.376	-14.33214	-0.0293685

Table 3.  
Dimensionless Aerodynamic Coefficient Calculation

Coefficient	Derivative to				
	u	$\alpha$	q	$\theta$	$\eta$
$X^*$	$\frac{C_{X_u} \rho V_0 S}{2m}$	$\frac{C_{X_\alpha} \rho V_0 S}{2m}$	$\frac{C_{X_q} \rho V_0 S \bar{c}}{4m}$	$\frac{C_{X_\theta} \rho S \bar{c}}{4m}$	$\frac{C_{X_{\delta_e}} \rho V_0^2 S}{2m}$
$Z^*$	$\frac{C_{Z_u} \rho V_0 S}{2m}$	$\frac{C_{Z_\alpha} \rho V_0 S}{2m}$	$\frac{C_{Z_q} \rho V_0 S \bar{c}}{4m}$	$\frac{C_{Z_\theta} \rho S \bar{c}}{4m}$	$\frac{C_{Z_{\delta_e}} \rho V_0^2 S}{2m}$
$M^*$	$\frac{C_{M_u} \rho V_0 S \bar{c}}{2I_{yy}}$	$\frac{C_{M_\alpha} \rho V_0 S \bar{c}}{2I_{yy}}$	$\frac{C_{M_q} \rho V_0 S \bar{c}^2}{4I_{yy}}$	$\frac{C_{M_\theta} \rho S \bar{c}^2}{4I_{yy}}$	$\frac{C_{M_{\delta_e}} \rho V_0^2 S \bar{c}}{2I_{yy}}$

computational fluid dynamic approach. Finally, after these parameters have been generated, the longitudinal dynamic equation of the aircraft can be arranged into a matrix, as shown in equation (1). This state matrix is constructed based on a single input of the elevator deflection angle.

$$\begin{bmatrix} \dot{u} \\ \dot{\alpha} \\ \dot{q} \\ \dot{\theta} \\ \dot{h} \end{bmatrix} = \begin{bmatrix} X_u & X_\alpha & X_q & X_\theta & 0 \\ Z_u & Z_\alpha & Z_q & Z_\theta & 0 \\ M_u & M_\alpha & M_q & M_\theta & 0 \\ 0 & 0 & 1 & 0 & 0 \\ 0 & -V_0 & 0 & V_0 & 0 \end{bmatrix} \begin{bmatrix} u \\ \alpha \\ q \\ \theta \\ h \end{bmatrix} + \begin{bmatrix} X_\eta \\ Z_\eta \\ M_\eta \\ 0 \\ 0 \end{bmatrix} \eta \quad (1)$$

The axial velocity is denoted as  $u$ , angle of attack as  $\alpha$ , pitch rate as  $q$ , pitch angle as  $\theta$ , altitude as  $h$ , and elevator deflection angle as  $\eta$ . The dimensionless aerodynamic coefficient is then substituted for equation (1) to construct the complete WiSE longitudinal dynamic equation as written in equation (2). This equation is derived based on the assumptions made in the previous section. It dictates the de-coupled longitudinal dynamic equation of the aircraft with a single input from elevator deflection angle and multiple-output (SIMO) associated with the longitudinal response of the aircraft. This equation is then applied to closed-loop control based on the pole placement and LQR methods to improve system performance.

$$\begin{bmatrix} \dot{u} \\ \dot{\alpha} \\ \dot{q} \\ \dot{\theta} \\ \dot{h} \end{bmatrix} = \begin{bmatrix} -0.0122149 & -0.0106271 & 0 & -9.81 & 0 \\ -0.00518525 & -5.28145 & 0.6270357 & 0 & 0 \\ -4.97107e-12 & 0.21405 & -3.19801 & 0 & 0 \\ 0 & 0 & 1 & 0 & 0 \\ 0 & -28 & 0 & 28 & 0 \end{bmatrix} \begin{bmatrix} u \\ \alpha \\ q \\ \theta \\ h \end{bmatrix} + \begin{bmatrix} 2.328277 \\ -3.73085 \\ -55.06689 \\ 0 \\ 0 \end{bmatrix} \eta \quad (2)$$

By using equation (2), we can analyze the dynamic stability response of the WiSE vehicle which consists of two modes, i.e., short period and phugoid mode. The short period mode has a higher damping ratio compared to the phugoid mode. This makes the short period mode have a shorter time to recover against the disturbance. On the other hand, the phugoid mode is used when a smooth variable transition is needed. The stability of an aircraft can be analyzed from the root locus diagram, which dictates the dynamic stability of the mode's characteristics. The root locus diagram of the original system can be seen in Figure 2. Based on the root locus diagram, the poles of the original system are

located at 0, -5.3442, -3.135, 0.02, and -0.0325. We can conclude that the system has unstable issues where a pair of poles move to the right side of s-plane as the gain value increases. Those poles represent the phugoid mode because of the low damping ratio, as stated before. Another instability issue occurs at the pole located at 0.02, which moves further to the right side of the s-plane with the increase of the gain value. This pole needs to relocate in order to eliminate the divergence response. In order to choose a suitable location for the new poles that meet the requirements, it is decided to observe the transient characteristics response of the system produced. This looks inconvenient since there is no exact rule to follow. However, a root locus diagram of the original system can be helpful in order to give insight for determining the location of the new poles. Based on this guidance, we can predict the transient behaviour of the system when several values of feedback gain are applied.

The poles located on the right side of the s-plane shows an unstable behaviour since the positive Eigenvalue will make the output to be divergent based on equation (3).

$$x(t) = e^{\lambda t}x(0) \quad (3)$$

where  $x(t)$  describes the state solution,  $\lambda$  is the Eigenvalue of the system,  $t$  is time, and  $x(0)$  is the initial condition of the system at  $t = 0$ . When  $\lambda$  is positive, the state response will go to infinite as time increases. Therefore, the poles on the right side of the s-plane need to be re altered to the left side using the pole placement or LQR methods. As mentioned before, in order to get the suitable gains feedback, it is needed to check the transient performances produced by varying several new poles location, i.e., maximum overshoot, settling time, etc.

### C. Altitude hold control

Maintaining the altitude of the WiSE vehicle is important to keep the advantages of the ground effect as it produces a high lift to drag ratio. By adding an altitude holding control, the vehicle is expected capable of maintaining its altitude always around 1 meter above the surface. The altitude holding control is designed using the pole placement method, where the gain constant  $K$  is used as the feedback control. The purpose of applying the pole placement method is to accelerate the system performance by forcing the origin pole location of the longitudinal dynamic equation into the desired

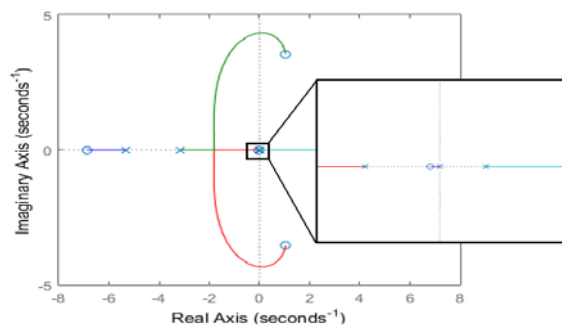


Figure 2. Root locus of the original system

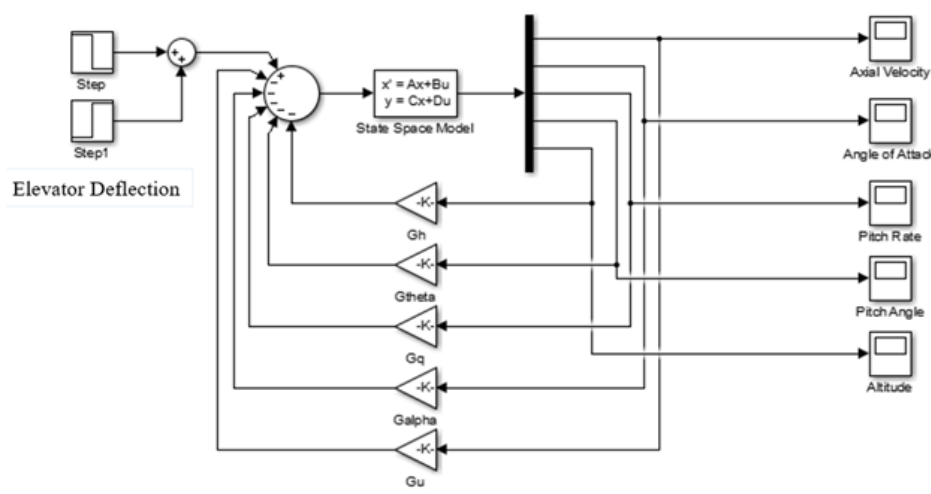


Figure 3. LAHCS block diagram using the pole placement method

location [16]. The WiSE longitudinal dynamic in equation (2) can be simplified as

$$\begin{aligned} \dot{x} &= Ax + Bu \\ y &= Cx \end{aligned} \tag{4}$$

where  $A$  is the longitudinal state matrix of the WiSE vehicle,  $B$  is the input matrix from the elevator,  $C$  is the output matrix,  $x$  is the state variable column matrix,  $u$  is the state variable input matrix, and  $y$  is the output column matrix. Let us assume that the input signal is

$$u = -Kx \tag{5}$$

where  $K$  is the state feedback gains matrix. Using this assumption, we can modify equation (4) to be

$$\begin{aligned} \dot{x} &= (A - BK)x \\ y &= Cx \end{aligned} \tag{6}$$

The system's response characteristics are determined by the Eigenvalues of  $A - BK$  matrix, which indicates the new systems pole locations. The root locus diagram from the initial system is used as a guide to find the pole locations that meet the

design criteria. It can be achieved by observing the transient response characteristics produced. In this paper, several variations of poles location are compared, and it is found that the pole locations that meet the design requirements are  $[-40 \ -1.9 \ -45 \ -40 \ -0.8]$ . The values of the gain matrix  $K$  are calculated using Ackermann's formula to give the feedback gain values stand at  $[-14600 \ 27400 \ -2470 \ -2500 \ -5140]$ , respectively. The dynamic response of the system with new poles location then tested against a step function and doublet input elevator using Simulink Matlab. The block diagram of the LAHCS and the longitudinal response of the system regarding the step input is shown in Figure 3 and Figure 4. We can see that the gains acquired from Ackermann's formula are implemented as feedback. The step function is implemented in order to extract the transient characteristics of the system, i.e., maximum overshoot, settling time, steady-state error, etc. [17] and [18]. Initially, the WiSE vehicle is assumed to fly on a steady level until a unit step input is implemented. This input will raise the response of the system, called the step response function. equation (7) describes the unit step input

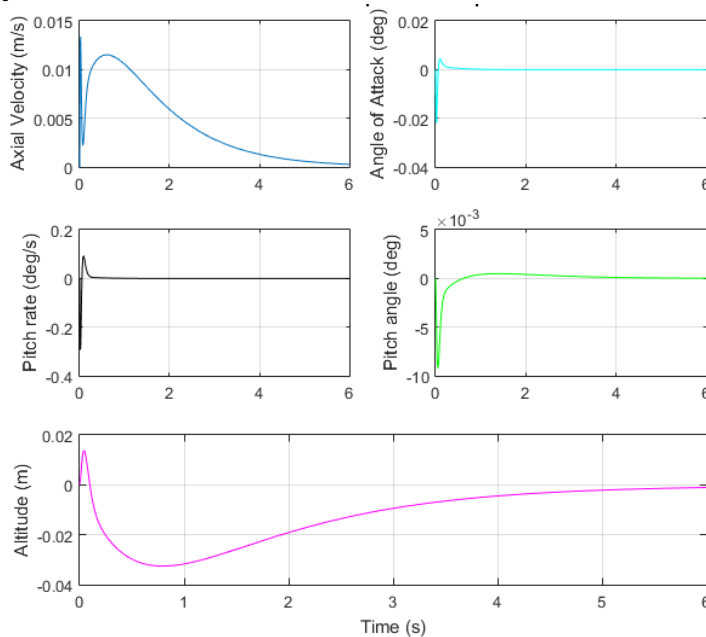


Figure 4. Systems response to the unit step input

applied to the close loop simulation.

$$s(t) = x_{SRF}(t) = \frac{1}{k} \left[ 1 - \frac{\alpha}{\beta} \sin\theta \right] \quad (7)$$

where:

$$\alpha = e^{-\xi\omega_n t}, \beta = \sqrt{1 - \xi^2}, \text{ and } \theta = \omega_d t + \varphi \quad (8)$$

$$\tan\varphi = \frac{\sqrt{1 - \xi^2}}{\xi} \quad (9)$$

where  $k$ ,  $\xi$ ,  $\omega_n$ ,  $\omega_d$ , and  $\varphi$  stand for stiffness constant, damping ratio, natural frequency, damped frequency, and phase angle respectively.

#### D. Altitude hold using LQR

In order to optimize the performance and the energy source of the system, the LQR method is applied by determining the weighting matrix of Q and R. Matrix Q deals with the performance of the system, while Matrix R is related to the cost factor. The Q matrix was altered to consider the axial velocity Q(1,1) and the altitude Q(5,5) of the WiSE vehicle. These two parameters are adjusted in order to achieve the good performance of the system by observing the response on the simulation results. The purpose of these alterations of the Q and R matrix is to minimize the cost function, represented as  $J = \int_0^{\infty} (x^T Q x + u^T R u) dt$ , which describes the area under the system response [12][19] and [20]. The detail of the Q matrix alteration is presented as equation (10):

$$Q = \begin{bmatrix} 100 & 0 & 0 & 0 & 0 \\ 0 & 1 & 0 & 0 & 0 \\ 0 & 0 & 1 & 0 & 0 \\ 0 & 0 & 0 & 1 & 0 \\ 0 & 0 & 0 & 0 & 5000 \end{bmatrix} \quad (10)$$

On the other hand, the R matrix is set at equation (11):

$$R = [0.1] \quad (11)$$

Using Ricatti's equation on equation (12), the LQR feedback gains can be determined as shown in equation (13)

$$A^T P + PA - PBR^{-1}B^T P + Q = 0 \quad (12)$$

$$K_{LQR} = R^{-1}B^T P \quad (13)$$

where B is the input matrix and P is the transformation matrix determined by solving the Ricatti's equation. Calculating using MATLAB program we get the LQR feedback gains matrix is

$$K_{LQR} = [0.31 \quad 837.8 \quad -62.1 \quad -1317.9 \quad -223.6]$$

### III. Results and Discussions

#### A. Control system response with pole placement method

Based on Figure 4, it can be seen that the system is dynamically stable with good transient characteristics. The altitude deviation is not exceeding the requirement, standing around 0.03 m, while the time needed for the aircraft to achieve a steady level is around 3.85 seconds. Table 4 summarizes the detailed response of the system regarding the unit step input.

The system then tested against the doublet input elevator to observe the robustness of the system in order to deal with a disturbance. To create the doublet input elevator profile, the elevator angle is set at  $5^\circ$  for 2 seconds, and then it is changed to  $-5^\circ$  for 2 seconds. Finally, the elevator angle is set back to  $0^\circ$  and maintain at that level. This scenario represents a severe disturbance and it will be worth it to examine the robustness stability of the system. The responses of the WiSE vehicle using the pole placement method due to the doublet input elevator are shown in Figure 5.

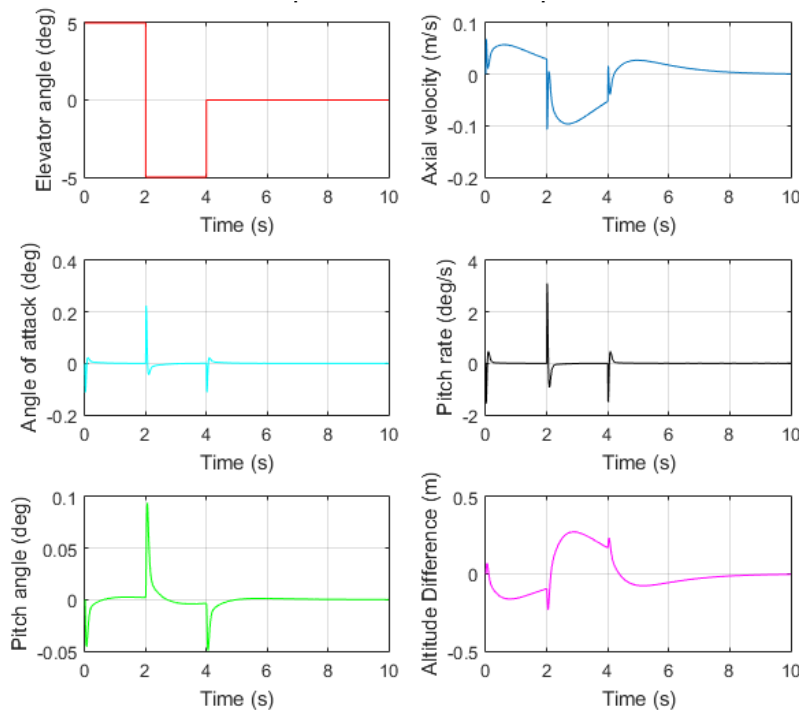


Figure 5. Systems response of doublet input elevator

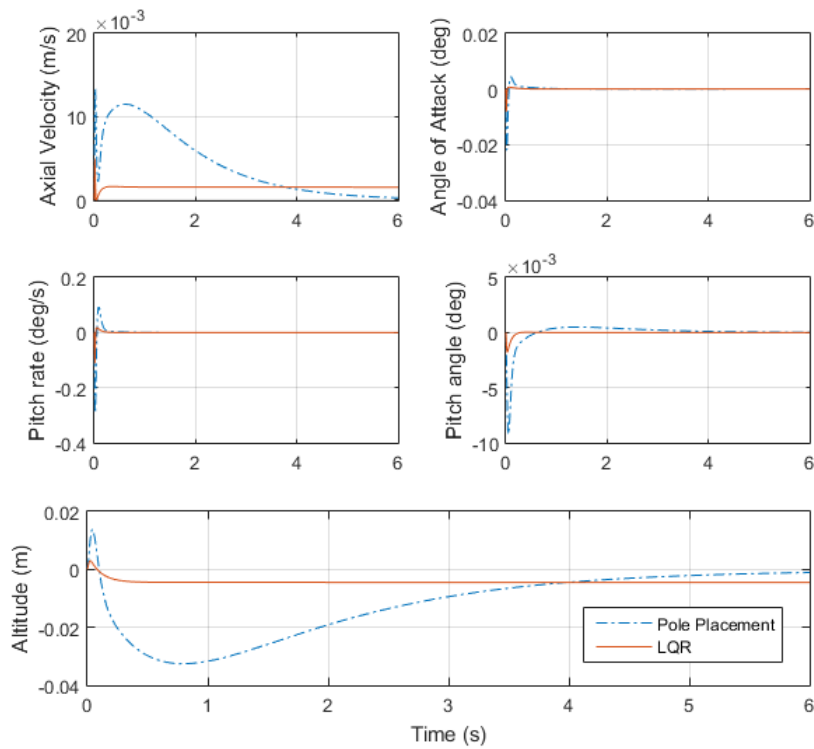


Figure 6. PP vs. LQR response of unit step input

The results seem convincing to comply with the requirement. It can be seen that the system's response due to the doublet input elevator has good transient characteristics, both for settling time and maximum deviation parameters. The angle of attack and pitch angle produced by the system's responses are not significant enough to cause a high altitude difference. Meanwhile, the maximum altitude deviation produced does not exceed 0.5 m, which stands at 0.272 m. It can be inferred that the pole

placement method is successful to generate a robust response to maintain the altitude always near the surface level. Detailed characteristics value from another response parameter can be seen in Table 5.

B. Control system response with LQR method

The comparison results between the pole placement and LQR methods regarding the unit step input and the double input elevator scenarios are shown in Figure 6 and Figure 7. It can be seen in

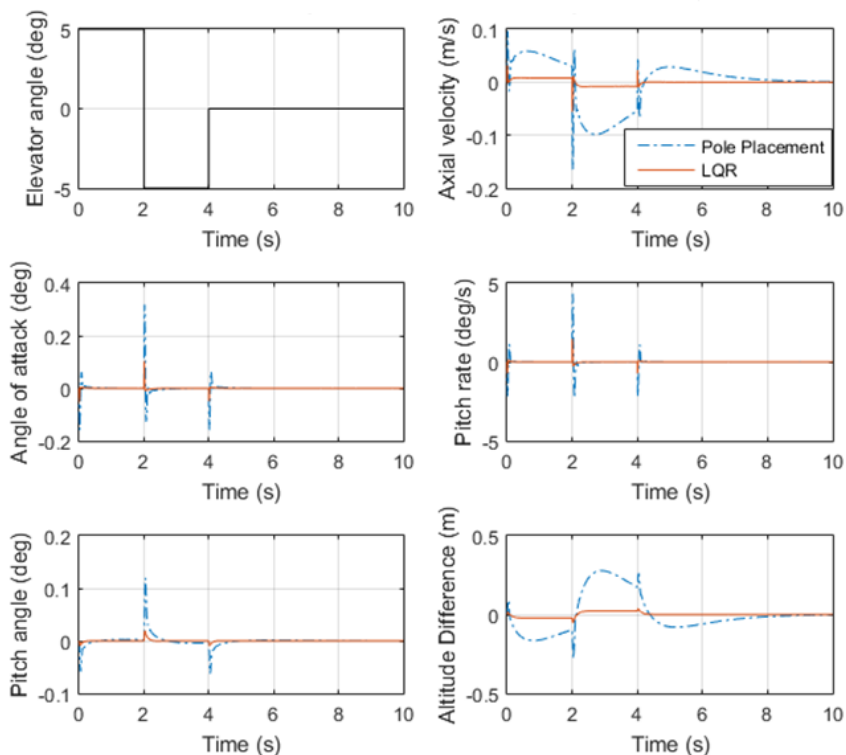


Figure 7. PP vs. LQR response of doublet input elevator

Table 4.  
Response of system to the step input

Parameter	Max. deviation	Settling time
Axial velocity	0.0134 (m/s)	2.28 (s)
Angle of attack	0.022 (°)	0.5 (s)
Pitch rate	0.2921 (°/s)	0.27 (s)
Pitch angle	9.24E-6 (°)	0.41 (s)
Altitude	0.03255 m	3.85 (s)

Table 5.  
Response of system to the doublet input elevator

Parameter	Max. deviation	Settling time
Axial velocity	0.1074 (m/s)	3.727 (s)
Angle of attack	0.2238 (°)	0.277 (s)
Pitch rate	3.11 (°/s)	0.219 (s)
Pitch angle	9.413E-1 (°)	0.423 (s)
Altitude	0.2723 m	2.246 (s)

Table 6.  
Response of LQR system to the doublet input elevator

Parameter	Max. deviation	Settling time
Axial velocity	0.0558 (m/s)	0.2 (s)
Angle of attack	0.1036 (°)	0.05 (s)
Pitch rate	1.47 (°/s)	0.28 (s)
Pitch angle	1.95E-2 (°)	0.24 (s)
Altitude	0.0552 m	0.24 (s)

Figure 6 that the LQR method reduces the altitude deviation of the system significantly, around 80 % in comparison with the response of the pole placement method. However, the settling time is quite similar between both systems.

Figure 7 informs that the LQR method response is better than the pole placement method for all parameters. However, the LAHCS using both pole placement and LQR method still meet the requirements and are capable of maintaining the altitude of the WiSe vehicle always near the surface. Detailed characteristics value from another response parameter can be seen in Table 6.

## IV. Conclusion

The LAHCS designed using the pole placement method can maintain the reference command altitude in which the settling time, maximum deviation, and delay time stand at 6.246 seconds, 0.27 m, and 0.198 seconds respectively. In order to improve the performance of the system, the locations of the new poles are defined at  $\lambda_{1\text{new}} = -40$ ,  $\lambda_{2\text{new}} = -1.9$ ,  $\lambda_{3\text{new}} = -45$ ,  $\lambda_{4\text{new}} = -40$ , and  $\lambda_{5\text{new}} = -0.8$ . The feedback gains obtained from Ackermann's formula based on the location of the new poles are  $K_1 = -1.46 \times 10^4$ ,  $K_2 = 2.74 \times 10^4$ ,  $K_3 = -0.247 \times 10^4$ ,  $K_4 = -2.5 \times 10^4$ , and  $K_5 = -0.514 \times 10^4$ . On the other hand, the LQR method is capable to reduce the maximum altitude deviation by around 80 % on the unit step input response, although the settling time response for both methods is similar. However, for the doublet input elevator response representing a severe disturbance, the LQR method could produce the most robust response for all parameters. To sum up, the LAHCS can maintain the altitude of the WiSe vehicle against

the disturbance and hold the altitude always near the surface for both of the methods applied.

## Acknowledgment

The authors thank the Department of Physics Energy Engineering, Surya University, for providing support and facilitation throughout the research. Special thanks to Mr. Andaro, who shared the design of the WiSe vehicle.

## Declaration

### Author contribution

All authors contributed equally as the main contributor of this paper. All authors read and approved the final paper.

### Funding statement

This research did not receive any specific grant from funding agencies in the public, commercial, or not-for-profit sectors.

### Conflict of interest

The authors declare no conflict of interest.

### Additional information

No additional information is available for this paper.

## References

- [1] R. Li and H. Chen, "The feasibility of high speed ground effect vehicles," *17th AIAA Aviation Technology, Integration, and Operations Conference*, 2017.
- [2] M. A. U. Amir and et al., "Wing in ground effect craft: a review of the state of current stability knowledge," *International Conference on Ocean Mechanical and Aerospace for Scientists and Engineer*, 2016.
- [3] S. Wiriadidjaja, A. Zahir, Z. H. Mohamad, S. Razali, A. A. Puaat and M. T. Ahmad, "Wing-in-Ground-Effect Craft: A Case Study in Aerodynamics," *International Journal of Engineering & Technology*, vol. 7(4), pp. 5-9, 2018.
- [4] H. Wang, C. J. Teo, B. C. Khoo and C. J. Goh, "Computational Aerodynamics and Flight Stability of Wing-In-Ground (WIG) Craft," *Procedia Engineering*, vol. 67, pp. 15-24, 2013.
- [5] M. M. Tofa, A. Maimun, Y. M. Ahmed, S. Jamei, A. Priyanto and Rahimuddin, "Experimental Investigation of a Wing-in-Ground Effect Craft," *The Scientific World Journal*, vol. 2014, 2014.
- [6] N. Kornev, "On Unsteady Effects in WIG Craft Aerodynamics," *International Journal of Aerospace Engineering*, vol. 2019, 2019.
- [7] Rahimuddin, A. Maimun, M. M. Tofa, S. Jamei and Tarmizi, "Stability Analysis of a Wing in Ground Effect Craft," *14th International Ship Stability Workshop*, Kuala Lumpur, 2014.
- [8] A. Nebylov and V. Nebylov, "Wing-in-Ground Effect Vehicles Flight Automatic Control Systems Development Problems," *Applied Mechanics and Materials*, vol. 629, pp. 370-375, 2014.
- [9] H. Muhammad, Sembiring, Javensius, Jenie and D. Said, "Development of Automatic Flight Control Systems for Wing in Surface Effect Craft," *IFAC Proceedings*, 2007.
- [10] W. Yang, Z. Yang and M. Collu, "Longitudinal Static Stability Requirements for Wing in Ground Effect Vehicle," *International Journal of Naval Architecture and Ocean Engineering*, vol. 7(2), pp. 259-269, 2015.
- [11] L. Parytta and M. N. Setiawan, "Design of UAV Longitudinal Regulator System Stability Due to Turbulence on Cloud Seeding Operation: A Case Study of Wulung PA-07," *7th International Seminar on Aerospace Science and Technology*, Jakarta, 2019.
- [12] E. Rizky and M. N. Setiawan, "Design of UAV Lateral Regulator System Stability Due to Turbulence on Cloud Seeding Operation: A Case Study of Wulung PA-07," *7th International Seminar on Aerospace Science and Technology*, Jakarta, 2019.

- [13] R. Finck and D. E. Hoak, "The USAF Stability and Control DATCOM" *Engineering Documents*, 1978.
- [14] Q. Qu, Z. Lu, P. Liu and R. K. Agarwal, "Numerical Study of Aerodynamics of a Wing-in-Ground-Effect Craft," *Journal of Aircraft*, vol. 51(3), pp. 913-924, 2014.
- [15] M. V. Cook, *Flight Dynamics Principles "A Linear System Approach to Aircraft Stability and Control Third Edition," Burlington, Ma: Elsevier, Ltd., 2012.*
- [16] K. Ogata, "Modern Control Engineering," *New Jersey: Prentice Hall*, 2010.
- [17] J. E. Cooper and J. R. Wright, "Introduction to Aircraft Aeroelasticity and Loads-Second Edition," *Chichester: John Wiley and Sons*, 2015.
- [18] R. Szabolcsi, "Pole Placement Technique Applied in Unmanned Aerial Vehicles Automatic Flight Control Systems Design," *land Forces Academy Review*, 23(1), pp. 88-98, 2018.
- [19] H. Purnawan, Mardlijah and E. B. Purwanto, "Design of Linear Quadratic Regulator (LQR) Control System for Flight Stability of LSU-05," *1st International Conference on Applied & Industrial Mathematics and Statistics*, Pahang, 2017.
- [20] A. Jafar and et al, "A Robust  $\infty$  H Control for Unmanned Aerial Vehicle Against Atmospheric Turbulence," *2nd International Conference on Robotics and Artificial Intelligence*, Rawalpindi, 2016.